Effects of structural relaxation, interdiffusion, and surface termination on two-dimensional electron gas formation at the LaAlO_{3}/SrTiO_{3} (001) interface

Ittipon Fongkaew, Sukit Limpijumnong, and Walter R. L. Lambrecht

Phys. Rev. B **92**, 155416 — Published 12 October 2015

DOI: 10.1103/PhysRevB.92.155416

Effects of structural relaxation, interdiffusion and surface termination on the two-dimensional electron gas formation at the $LaAlO_3/SrTiO_3$ (001) interface

Ittipon Fongkaew,[1,2,3] Sukit Limpijumnnong, [2,3] and Walter R. L. Lambrecht.[1]
[1] *Department of Physics, Case Western Reserve University, Cleveland, OH 44106-7079*
[2] *School of Physics and NANOTEC-SUT Center of Excellence on Advanced Functional Nanomaterials, Suranaree University of Technology, Nakhon Rachasima, 30000 Thailand and*
[3] *Thailand Center of Excellence in Physics(ThEP Center), Commission on Higher Education, Bangkok 10400, Thailand*

First-principles (generalized gradient approximation) calculations are presented for symmetric $LaAlO_3/SrTiO_3/LaAlO_3$ [001] orientation slab models with varying thickness (3, 4, 5 unitcells) of the $LaAlO_3$ (LAO) layers. The buckling of the layers and their effect on the slope of the layer averaged electrostatic potential and layer projected densities of states are studied. We find the buckling of the LAO layers to increase from the interface toward the surface, while the buckling of the AlO_2 layers decreases toward the surface. The critical layer thickness for obtaining electrons in the Ti-*d* band of the STO is determined to be 4 layers within this model. Beyond this point, the sloped potential is confined to the 4 layers of LAO nearest to the interface. The electrons in the Ti-*d* states extend throughout the 5.5 layer thick STO region of our calculation. The sheet charge density of electrons in the STO conduction band is determined and found to be of order $1-3\times10^{13}$ e/cm^2, in fair agreement with experimental values and an order of magnitude smaller than required by the polar discontinuity model. We also find still a significant change in the sheet density between the 4-LAO layer and 5-LAO layer model. It results in only d_{xy}-like states being occupied for the 4-LAO layer case but other t_{2g} bands becoming occupied for the 5-LAO layer case. The effects of H adsorption on surface O and OH adsorption on the surface Al are investigated for a model with 1/8 coverage of H and 1/4 coverage of OH. The former leads to electron doping of the $SrTiO_3$ (STO) layer while the latter leads to a p-type surface. When both together are present, they cancel each other. For high H-coverage, we find that only a certain fraction of the electrons donated by H can be accommodated at the interface while the remaining go to the surface and lead to a reversal of the slope of the potential in the LAO region. Addition of 25 % Ti on Al sites into the first layer of LAO, already leads to a cancellation of the field in the LAO layer. It does not lead to Ti^{3+} embedded in the LAO site but rather the Ti donates its additional electron to the interface 2DEG confined to the STO TiO_2 layers. A swap of Al with Ti in the layers closest to the interface does not produce a 2DEG because the Al in the TiO_2 interface layer provides holes compensating the electron doping from the Ti. Interdiffusion of Sr and La between the layers nearest to the interface does not lead to a 2DEG. These species are just electron donors in their own materials respectively. In a swap compensating dipoles result from the different nuclear charges but the electronic states near the gap are not affected. Thus no 2DEG formation occurs. On the other hand a Sr_{La} placed in the middle of the LAO layer is found to facilitate electron transfer from the surface to the interface and could lead to a 2DEG. However, the latter had only a small sheet density.

PACS numbers: 73.20.At

I. INTRODUCTION

The two-dimensional electron gas (2DEG) formation at the $LaAlO_3/SrTiO_3$ (or LAO/STO) interfaces has received enormous attention since its discovery by Ohtomo and Hwang.[1] Several mechanisms have been proposed for this phenomenon: (1) electronic reconstruction to avoid the polar discontinuity, (2) oxygen vacancies in the STO or LAO layers, (3) interdiffusion of Ti or Sr into the LAO layer and vice versa, or combinations of the above mechanisms. It is now well established that the role of oxygen vacancies in the STO depends strongly on the growth conditions, in particular the oxygen partial pressure during pulsed laser deposition. However it can be controlled by annealing and is assumed to make a negligible contribution for sheet carrier densities of order 10^{13} e/cm^2. There has also been ample evidence for some degree of interdiffusion, most recently through a Medium Energy Ion Scattering (MEIS) study by Zaid *et al.*[2]. The gradual change in c/a ratio observed in these measurements could be well explained by models including a gradually changing interdiffusion model.

The original polar discontinuity model[1] is based on the idea that in STO each layer SrO or TiO_2 is neutral but in LAO the nominal charge per unit cell alternates between -1 for the LaO and $+1$ for the AlO_2 layers. This discontinuity would set up a field with an ever increasing potential in the LAO layer, until the potential difference exceeds the band gap and charge is transferred from the surface to the interface. Within this model, a net charge of 1/2 electron per unit cell corresponding to about 3×10^{14} e/cm^2 is required at the interface to cancel the field. On the other hand, experimentally one usually finds a significantly lower charge density. This model also predicts a corresponding hole gas at the surface, which has not been observed. Evidence for a sloped

potential in the LAO region has not been established conclusively experimentally either. While in principle explaining the presence of a critical layer thickness for observing a 2DEG, the quantitative determination of the critical layer thickness is complicated by the possibility of relaxation of each layer,[3,4] the fact that the gap is underestimated by the usual semi-local density functional calculations, and so on. Janotti and Van de Walle[5] took a somewhat different viewpoint assuming that the discontinuity is immediately met at the interface by the interface bond configuration but proposed that the interface charge may subsequently be partially transferred to the surface depending on the configuration considered and the surface passivation. They used this model to address the question why less than 1/2 electron per unit cell area is often found at the interface. Other possible explanations are that part of the charge at the interface is not detected in transport because it resides in less mobile interface states.[6] A related question is why a 2D hole gas is not observed at the surface. Several possibilities have been offered for this asymmetry between the n- and p-type interface.[5,7,8] Another possibility is that the holes form self-trapped polarons in these oxides.[9]

It is by now more or less accepted that the above mentioned mechanisms are not mutually exclusive but may each contribute to the 2DEG formation to a varying degree depending on growth conditions and so on. The role of defects has been addressed recently by Yu and Zunger.[10] They explained the occurrence of a critical layer thickness in terms of the energy of formation of oxygen vacancies on the LAO surface which becomes negative when the layer exceeds a critical thickness. However, this dependence of the energy of formation of the V_O on the position of the V_O relative to the interface results itself from the sloped potential, as was pointed out in several earlier papers[8,11,12]. However Yu and Zunger proposed that the discontinuity for thicknesses below the critical thickness is already removed by the antisite defects of Ti on Al sites at the surface transferring its electron to an Al on Ti sites across the interface on the STO side. So, it is then not clear why V_O would still form at the surface if interdiffusion is already removing the sloped potential.

On the other hand, in the classic polar catastrophy explanation, the slope in the LAO region is not removed since the Fermi level becomes pinned slightly below the valence band maximum (VBM) of the AlO_2 surface layer of LAO and slightly above the conduction band minimum (CBM) at the STO (TiO_2) interface layer. Lee and Demkov[13] claimed that the polar catastrophe model could quantitatively explain the charge density at the interface. Using the LDA+U method, they found that it resides in interface states of the Ti below the STO CBM.

The surface termination is also known to play an important role. This is most clear from the experiments by Cen *et al.*[14–18] in which it was shown that regions of 2DEG at the buried interface can be induced by modifying the surface adsorbates with an appropriately biased atomic force microscopy (AFM) tip.

The literature on the LAO/STO at this point in time has become too extensive to review comprehensively, so the above is only a sampling of the key ideas relative to the origin of the 2DEG. In this paper, we first revisit the original polar catastropy idea by modeling LAO overlayers on STO of various thickness and studying both the ionic relaxations, the partial densities of states and the planar averaged electrostatic potential profile. We determine quantitatively the interface sheet carrier density in the conduction band of the STO and interface region. These results are presented in Secs.III A and III B. Subsequently, we study the effects of surface termination with H, OH and both together in Sec. III C. Next, we consider interdiffusion of Ti-Al and Sr-La in sections III D and III E. Interdiffusion of Ti and Al side in the near interface layers was recently observed by MEIS.[2] These various models clarify the behavior of the interface charge density and the way in which the polar catastrophy, or more precisely the slope in electrostatic potential, is mitigated and are a step along the way to build a quantitative model for determining the relative contributions of each type of mechanism. The main conclusions of our study, highlighting what we believe are new findings, are summarized in Sec.IV. Before we present our results, a brief description of our computational models and methods is given in Sec. II.

II. COMPUTATIONAL METHOD

The calculations are carried out within the framework of density functional theory and using a plane wave basis set with projector augmented wave potentials (PAW)[19,20] using the VASP code[21–23]. The PBE-GGA approximation is used for the exchange correlation potential.[24,25] The electron wave functions were described using a plane wave basis set with the energy cutoff of 500 eV. This energy cutoff is sufficient to provide a well-converged basis set to describe oxides when using ultrasoft pseudopotentials.[26]

To study LAO/STO(001)interface, the supercells were set up in a symmetric way with 5.5 (001) oriented STO layers (meaning 6 TiO_2 layers and 5 SrO layers) and either 3, 4, or 5 unit cell LAO layers on either side, followed by 20 Å of vacuum. This allows us to include the surface effects with different terminations. We focus exclusively on the TiO_2/LaO interface, which is the n-type interface in which the 2DEG is experimentally observed. Several previous studies have also considered the SrO/AlO_2 p-type interface, for example Ref. 8 and references therein. The symmetric geometry with two identical interfaces is chosen so as to avoid spurious fields from the periodic boundary conditions. The thickness of the vacuum region is sufficient to avoid spurious slab-slab interactions. For the first part of the study we pick a 1×1 2D surface cell. For the surface adsorption studies or the interdiffusion models we choose a 2×2 2D cell. In that case, the

surface AlO_2 layer has 8 O atoms, and 4 Al atoms. Thus, we can go down to a H surface concentration of 1/8 and OH concentration on Al of 1/4. Additional calculations with full surface coverage were done on the 1×1 surface cell. Similarly for the interdiffusion we also used a 2×2 2D cell, so that we can model for example a 25 % Ti, 75 % Al layer. In addition, we can choose to simply add Ti instead of Al or swap Al and Ti from the STO to the LAO side of the cell and we can choose which layer to place the swapped atoms in: closer to the interface or further away. Similar considerations apply to Sr-La interdiffusion. The actual models studied will be presented along with the results.

For structure relaxation, the in-plane lattice constant of the slab was constrained at the calculated value of STO bulk ($a = 3.8695$ Å). All coordinates of atomic positions were fully relaxed until the residual Hellmann-Feynman forces[27] become less than 0.02 eV/Å. For k-space integrations, we used the Monkhorst-Pack scheme[28] with 7x7x1 k-point sampling.

III. RESULTS

A. Structural relaxation in models without interdiffusion

We start by examining the ionic relaxation as function of LAO overlayer thickness. These results are shown in Fig.1 We present the results as a buckling of the mixed cation anion layers, in other words, the relative z coordinate (normal to the (001) planes) of the cation minus that of the anion in each layer. One may see that, in agreement with early results of Pentcheva and Pickett,[3,4] the surface AlO_2 layer remains unbuckled. However, as we approach the interface, the AlO_2 layer buckling increases. On the other hand, the buckling of the LaO layers is stronger and is reversed: it increases toward the surface although not entirely linearly with distance from the interface. We note that the displacement of positive cations toward the surface relative to the negative anions, means that dipoles in each layer are formed which counteract the slope of the potential. Thus the potential slope, resulting from the valence discontinuity, is in part avoided by relaxing the layers.

B. Electronic structure in models without interdiffusion

Next, we consider the layer projected densities of states in Fig.2. We can see that for the 3-LAO layer case, the layer projected density of states (PDOS) in the LAO are shifted from layer to layer displaying the expected electric field from the polar discontinuity. This sloped potential leads to a strong decay of the states near the top of the valence band in the LAO away from the surface. This occurs over about a 1 eV range below the surface VBM. It

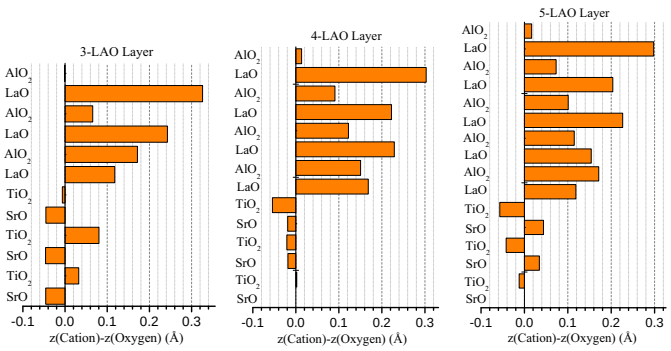

FIG. 1. (Color on-line) Buckling of layers in LAO/STO models: The bar graphs show $\Delta z = z_{\text{oxygen}} - z_{\text{cation}}$ with z the distance normal to the interface and positive toward the surface.

shows that the LAO VBM becomes almost like a surface state and reflects simply the band bending.

The VBM of the surface LAO in the 3-LAO-layer, however, stays below the CBM of the STO and hence no charge transfer occurs between the two. For the 4 layer and 5 layer cases there is a charge transfer. One can also see that the charge density in the STO is spread over all TiO_2 layers in our model. So, it is spread out over several layers near the interface. In Fig. 2 we show the results only for the 3-LAO and 5-LAO layer cases. Those for the 4-LAO layer case look similar to the 5-LAO layer case but with the Fermi level slightly closer to the STO CBM in the interface layer. We see no evidence for a localized interface state splitting off below the CBM in these figures.

We also examined more closely if an interface state occurs at the interface by performing spin-polarized calculations. In that case, we find for the 5-LAO layer case, a separate small peak in the PDOS for majority spin. This is shown in Fig. 3. It agrees qualitatively with the conclusions of Lee and Demkov.[13] These authors used LSDA+U in which the Hubbard U further shifts the occupied interface state down into the gap. We see that this already occurs without Hubbard U. In other words by placing a small amount of charge in the bottom of the conduction band it becomes favorable to induce a magnetic moment by splitting the up and down spin bands. The total magnetic moment of the cell was found to be 0.12 μ_B for the 5 -layer 0.08 μ_B for the 4-LAO layer case. This corresponds to two interfaces, so per interface the values should be halved. This occurrence of a weak magnetization is somewhat surprising because the density of states near the conduction band minimum is not very high, so one would not expect the Stoner criterion to be fulfilled. In fact, for the 4-LAO layer case, the up and down spin PDOS stay essentially the same but for the 5-LAO layer case, a sharper interface state of only majority spin splits off.

Next, we determine the interface sheet electron density

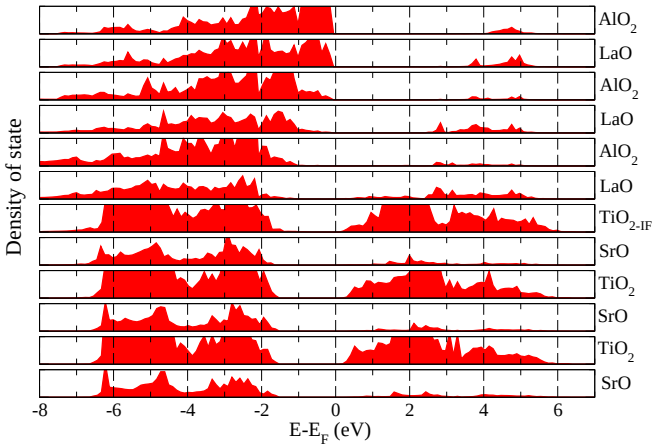

(a)

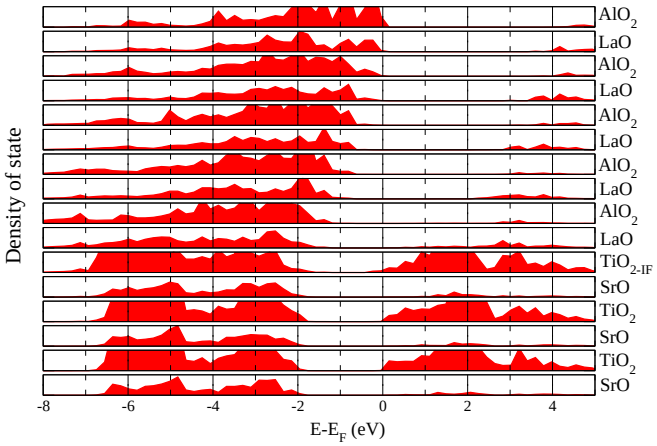

(b)

FIG. 2. Layer-projected density of states of (a) 3-LAO layer and (b) 5-LAO layer layer

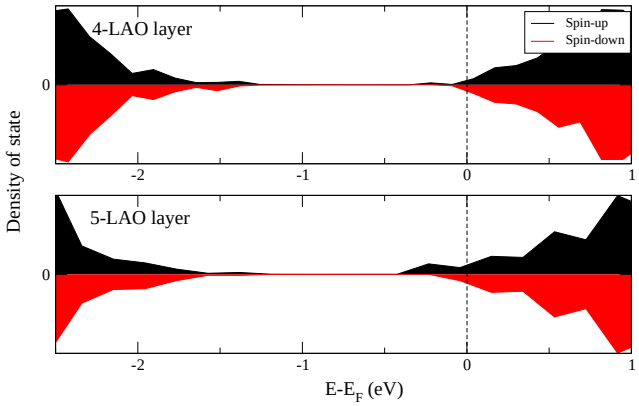

FIG. 3. Layer-projected density of states, focus on interface layer of 4 and 5 LAO layer, including spin-polarization.

of free carriers in the STO conduction band. The conduction band 2D charge densities at the interface were determined by first extracting the charge density accumulated only over states from some level in the gap up to the Fermi-energy, then planar averaging it over the xy planes parallel to the interface and then integrating only over the layers near the interface and in the STO region. This is illustrated in Figs. 4 and 5.

In Fig. 4 we show a 3D plot of the structure with the electron density integrated between a lower energy limit E_a chosen in the gap and the Fermi energy E_F. As can be seen this charge density has a large contribution near the free surface. This is because E_a cuts through the LAO valence band PDOS near the surface. Here, we would actually be rather interested in the hole density, i.e. the integral from the Fermi level to an upper level above the local VBM.

For our present purpose of determining the interface electron density, we next planar average it over xy planes as shown in Fig. 5 and simply integrate over z only over the middle region from about 50 Å to 75 Å. The zero of the distance perpendicular to the layers is chosen in the middle of the vacuum region. In practice, we include only the layers in LAO where the lower energy limit already lies above the VBM. However, it does include the whole STO region and thus gives truly the sheet density whether it is localized near the STO interface or spreads out over a few STO layers. The resulting net sheet densities are 1.43×10^{13} and 2.14×10^{13} e/cm^2 for the 4-LAO layer and 5-LAO layer cases respectively. These are in good agreement with experimental values of Thiel et al.[29] and indeed much smaller than the nominal charge of 1/2 e per interface unit cell area as assumed in the polar discontinuity model. From Fig. 5, only shown for the 4 layer case, we can also see that the charge density is slightly higher near the interface but decays rather slowly into the STO region.

Returning to Fig. 4 we may notice that the charge density also provides information on the orbital character of the interface charge. In the 4-LAO layer case, it clearly consists of d_{xy} like states throughout the STO region. In the 5-LAO layer case, the isosurfaces inside the STO look more cubic, because now the d_{xz} and d_{yz}, *i.e.* the other t_{2g} orbitals also contribute. This is related to the fact that we have a significantly higher interface sheet density in the 5-LAO layer case. In fact, the thin STO layer confinement effects are more strongly affecting the d_{xz} and d_{yz} states than the d_{xy} states. Thus, for low carrier concentration, we only fill the d_{xy} bands, while for the higher concentration we start to fill both but near the interface, the states are still predominantly d_{xy} like. Similar observations on the nature of the interface states were made in Ref. 6.

Next, we also examine the layer averaged electrostatic potentials (in Fig. 6.) and examine the slope in the LAO layer. This gives a field of 0.21 eV/Å for the 3-layer case. Within the framework of the polar discontinuity model, this field should be given by $E = 4\pi\sigma/\varepsilon$. Using a static dielectric constant of $\varepsilon = 28$ from Ref. 30 this gives a $\sigma = 3.2 \times 10^{14}$ e/cm^2, as expected from the discontinuity model. This charge results from the total nuclear plus

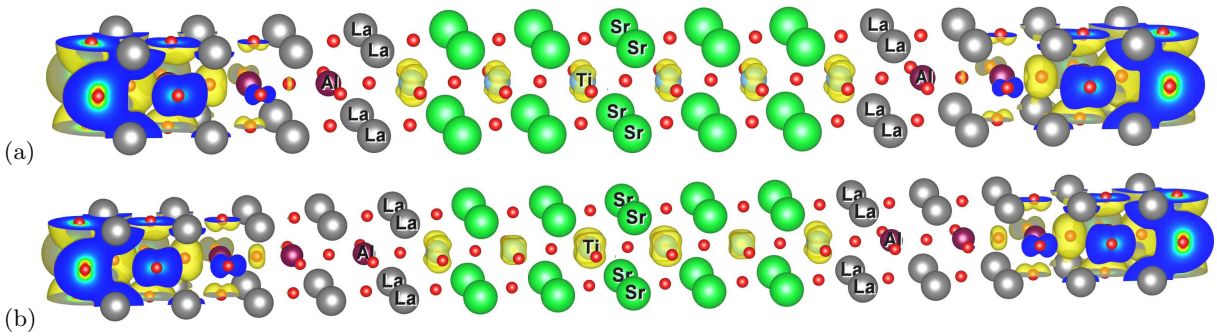

FIG. 4. (Color on-line) Structure and charge density in energy range between STO middle of the gap and Fermi energy (3D plot) for (a) 4-LAO layer and (b) 5-LAO layer, respectively. The yellow surface is an isosurface of the charge density, the blue shows the inside of this surface where the unit cell cuts through it.

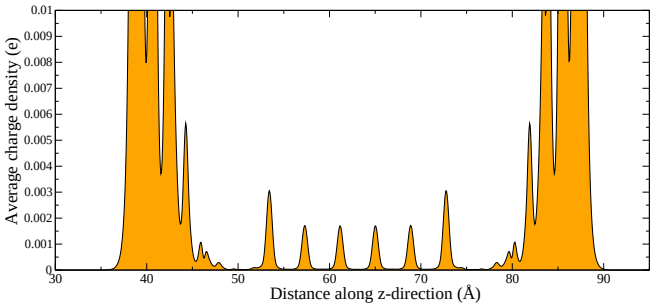

FIG. 5. (Color on-line) Charge density in energy range between STO middle of the gap and Fermi energy averaged over the xy plane for the 4-LAO layer model.

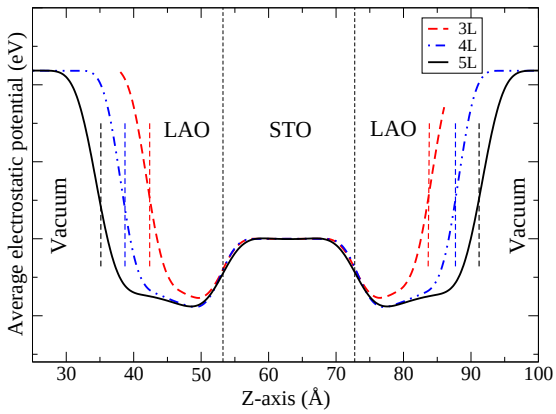

FIG. 6. (Color on-line) Macroscopically averaged electrostatic potentials of the 3-, 4- and 5-LAO layer cases. The potentials are averaged over the xy plane and filtered by a running average in the z-direction to filter out layer by layer variations. The vertical dashed lines show the position of the O in the TiO_2 interface layer and the position of the O in the AlO_2 surface for each case are marked by short vertical dashed lines.

electronic charge and reflects the true discontinuity in electric field arising from the juxtaposition of nominally alternatingly positive (LaO) and negative (AlO_2) layers on top of the STO neutral layers. However, we see that once the gap is closed and some charge is transferred from the surface to the interface as in the 4 and 5 layer cases, the slope is reduced. However, it is not reduced to zero as is also clear from the PDOS in Fig. 2. This is consistent with the significantly lower conduction band interface charge or sheet density we found above. Part of the potential slope is reduced also by the dipoles resulting from the ionic displacements discussed in the previous section.

Furthermore we can see that near the interface, the slope in the 5 layer case is similar to the 4 layer case but the potential then flattens out as we approach the surface. In that sense the somewhat larger net interface charge indeed avoided the polar catastrophy. If one would add more layers of LAO, presumably the sloped potential region would only occur near the interface after which the potential would remain flat. In the present case, the next layer is however already close to the surface where another dipole potential obviously is present to the vacuum level outside the layer.

The above detailed analysis clarifies what actually happens in the purely electronic reconstruction model in terms of "avoiding the polar catastrophe".

C. Surface terminations

Next we consider the effects of surface terminations. In Fig. 7(a) we show the layer by layer PDOS for a 2×2 cell with one H on the surface O in the AlO_2 surface layer. This means it corresponds to a 1/8 surface coverage with H. A structural model of the surface configuration is included at the top of the figure. The PDOS shows that the H forms bonding and antibonding states with the surface O-2s and O-2p. We can see these H bonding below the O-2p band at -8 eV. The ones below the O-2s occur at -21 eV just below our energy range cut-off and are thus not visible in the figure. The corresponding antibonding state lies high in the conduction band. There are however, no extra states below the Fermi energy near the surface. Thus the additional electron from H finds its way to the lowest available empty states which are at the

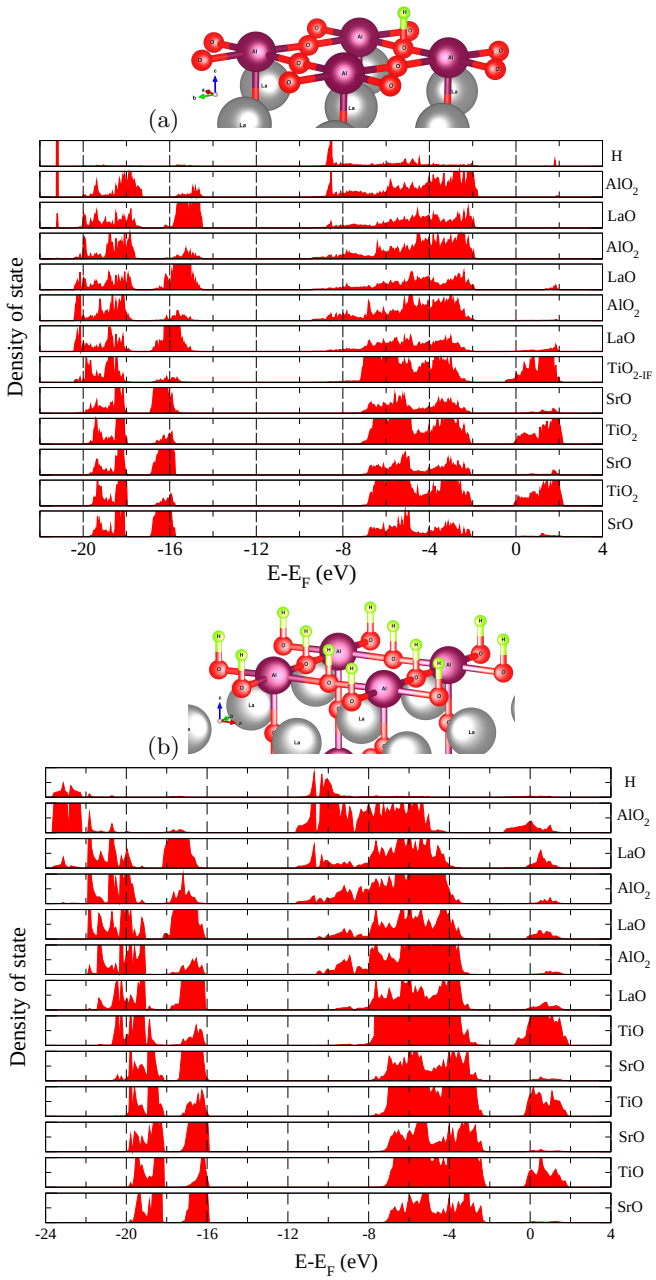

FIG. 7. (Color on-line) Layer-projected density of states and their surface structure in case of (a) 1/8 H atom coverage and (b) full coverage by H atoms, respectively.

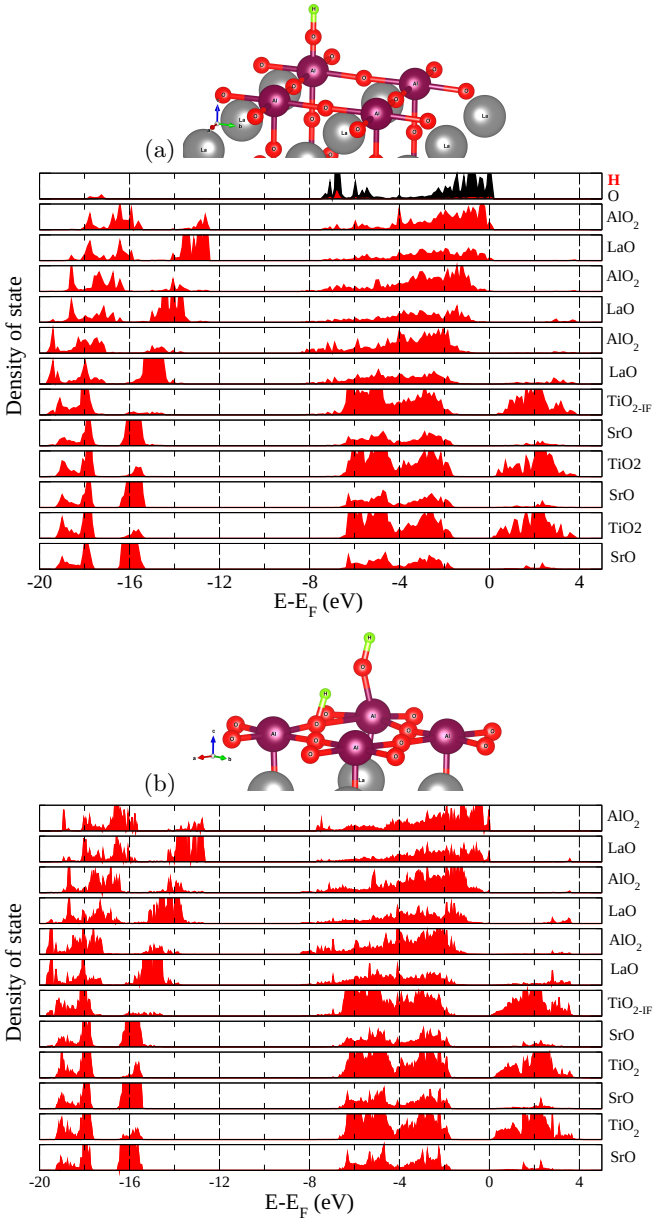

FIG. 8. (Color on-line) Layer-projected density of states and their surface structure in case of surface partially covered by (a) OH and (b) H_2O(dissociated in to OH and H), respectively.

CBM of STO in the TiO_2 layers. These calculations were performed for an LAO thickness of only 3 unit cells. In other words, even below the critical thickness covering the LAO surface with a hydrogen coverage of only 1/8 already provides the necessary charge for eliminating the polar catastrophe. In fact, the slope in the potential on the different LaO or AlO_2 layers is seen to be almost zero. In this case, the charge density at the interface determined as explained in the previous section is 1.20×10^{13} e/cm^2. On the other hand, we also studied a full coverage of H using the 1×1 2D cell model. In that case, we find that the interface charge increases only to 3.01×10^{13} e/cm^2. However, there is now a significant charge density near the surface. This is shown in Fig. 7(b). In fact, in this case the polar catastrophe is overcompensated. One may now see that the potential slope is reversed and the potentials shift down from the interface to the surface. This leads to a downward shift of the the LAO conduction band, which now also becomes partially filled. This implies that we now would have both the surface and interface layers to become conducting. The electrons den-

sity in the surface layer was also determined in a similar manner as the interface and amounts to 6.2×10^{13} e/cm^2. This calculation for full H coverage was also repeated for a 4-LAO layer model. Similar results are obtained but now the 2DEG sheet density increased to 9×10^{13} e/cm^2. This indicates that the H effects are accumulative with the charge already there from surface to interface charge transfer. For 3-LAO layer model with a half H coverage we obtain 2.88×10^{13} e/cm^2.

These results indicate that even a small amount of H adsorption on the surface is sufficient to eliminate the potential slope. The interface 2DEG density can be further increased in proportion to the H concentration. However the interface 2D electron gas sheet density cannot be increased much beyond the 10^{13} e/cm^2 level without overcompensating the fields and creating an opposite polar catastrophe, which now also leads to a surface conducting layer.

Next, we consider OH attached to the surface Al. Again, this is done for the 2×2 2D cell and 3 layers of LAO. The result is is shown in Fig. 8(a). It leads to a surface state just above the VBM which stays empty. This can be explained as follows. We add 8 states for the O-2s and O-2p below the VBM but we add only 7 electrons. So, the Fermi level crosses through the VBM or rather between the VBM and the surface state which then becomes a p-type surface. However, we still have a strongly sloped potential and no electrons in the interface, so no 2DEG formation. As expected, when we have one of each, OH and H, (as shown in Fig. 8(b), the two effects compensate each other and we obtain essentially the same sloped potential as before for the bare surface for the 3-LAO layer case, *i.e.* no 2DEG formation at the interface.

These results are relevant for the surface modification effects as studied by Cen *et al.*[14,18] These authors proposed a model for their AFM tip surface manipulation studies. The assumption is that in the native state, the surface is covered by equal amounts of H and OH resulting from water in the atmosphere which is split and adsorbed separately as OH on Al and H on surface O. Our calculations indeed indicate that the total energy for H_2O adsorbed on an Al is higher than an OH and H separately adsorbed on Al and surface O respectively by 1.8 eV per H_2O molecule. This is obtained from separate studies of OH and H and H_2O adsorption on a pure LAO slab. For absorption on the LAO/STO/LAO slab we find a somewhat smaller but still positive energy of 0.6 eV. Thus the interface seems to have some effect on this reaction energy. However, in any case the separate adsorption of H and OH and splitting of the water molecule is preferred.

One may now assume that the tip removes OH and thereby activates locally the H to donate its electrons to the interface and create locally a 2DEG. Interestingly, our present calculations indicate that this by no means requires a full coverage of the surface with H_2O. In fact, a full coverage of the surface with H would overcompensate the polarity discontinuity field. Further experimental work to elucidate the actual surface coverages with H and OH in dependence on the partial pressures in the gas would be quite interesting. At present we cannot yet fully quantitatively determine what the maximum 2DEG carrier concentration is that is achievable in this way. It is also unclear if the same effect would add to the 2DEG charge density at the interface if the starting system with compensated H and OH is already above the critical layer thickness. Our one calculation for a 4-LAO layer and full H coverage indicates the effects are accumulative.

D. Ti-Al interdiffusion effects.

In this section, we consider various effects of interdiffusion. First we start with replacing one Al in the first LaO layer next to the interface by Ti in the 2×2 2D supercell. After relaxing the structure, we found that the Ti was slightly displaced away from the interface. This agrees with observations by Zaid *et al.*[2]. This can be seen in the structural panel (left) and buckling panel (middle) in Fig. 9.

The effect on the PDOS can be seen in the right panel of Fig. 9. The macroscopically averaged electrostatic potential is shown along with that of other cases, to be discussed below in Fig. 10. The potential for the case of an added Ti_{Al} in the first AlO_2 layer is shown by the red-dotted curve, labeled Ti_{Al}. While potential slopes in this curve remain visible near the interface and near the surface, compared with the no interdiffusion case (solid line), the potential in the central region of the LAO layer now looks flat, whereas it had a monotonic slope toward the surface in the abrupt interface case without interdiffusion. One could conclude that the added Ti_{Al}, *i.e.* a 4-valent atom on a 3-valent site, had the effect of compensating the valence discontinuity at the interface. The remaining slopes near the surface are also clearly seen in the PDOS in Fig. 9. The Fermi level lies above the STO CBM. We can see that the Ti in the mixed layer however did not produce a defect level in that layer. The Ti like PDOS in this layer lies well above the Fermi level with peaks at about 1 eV above the Fermi level and it has donated its electron to the interface. This implies that the interdiffused Ti_{Al} did not convert to Ti^{3+} as is often assumed. Instead because of the higher electrostatic potential of this layer, it turned out to be preferable to let this extra electron move to the interface. So, in some sense it contributes to the electronic reconstruction. Only, instead of the charge coming from a p-type surface it came from the Ti_{Al} site in the mixed LaO interface layer. The sheet density of the 2DEG in the interface in this case is 1.1×10^{13} e/cm^2.

We now consider the PDOS in Fig. 9 in the four topmost layers starting from the surface. We here see a decreasing PDOS in the energy range -1 eV to -2 eV from the surface inward. These states persist all the way down to the first LaO layer above the mixed Ti-AlO_2 layer but

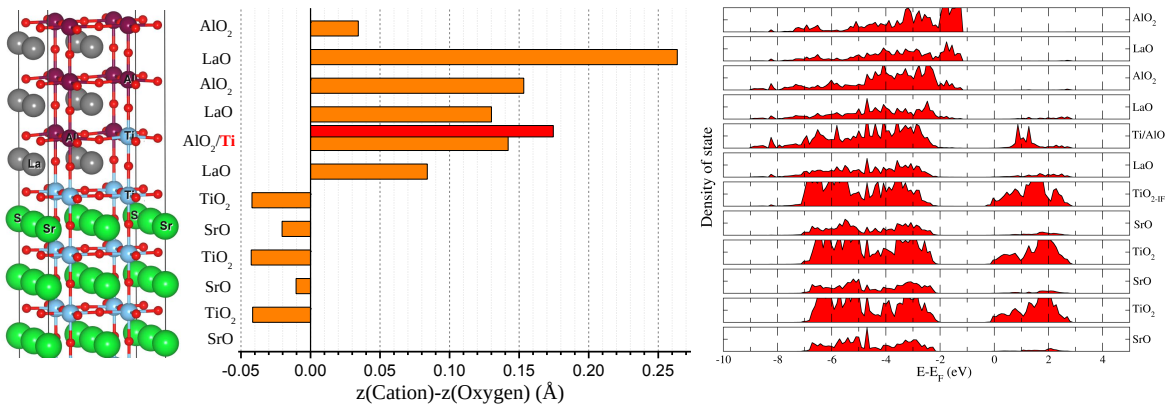

FIG. 9. (Color on-line) Structural model (left), buckling of layers ($z_{\rm cation} - z_{\rm oxygen}$) (middle), and PDOS (right) for the 25 % Ti 75 % Al layer model. For the mixed layer, the Ti displacement is indicated in red, the Al displacement in orange as indicated.

are not present in the LaO layer near the interface. In that sense there is an abrupt change in the upper valence band state of the second and third LaO layer (counting down from the surface). It looks in other words, like a localized surface state. This is similar to the models without interdiffusion discussed in section III B. In some sense, what the added Ti did was shift the interface closer to the surface so it is now only two LAO-layers below the surface instead of three. This slope in potential over the near surface layers can also be seen in Fig. 10.

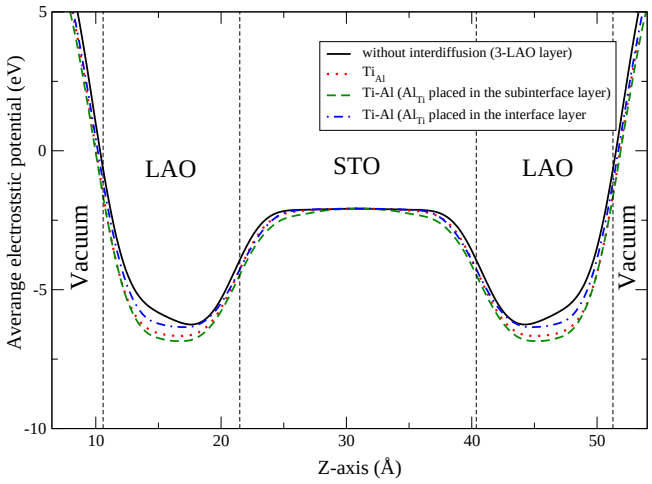

FIG. 10. (Color on-line) Macroscopically averaged electrostatic potentials for three Ti-Al interdiffusion models compared with the case of no-interdiffusion. The vertical dashed lines show the position of the surface and interface layers.

Next, instead of adding Ti, we studied swapping a Ti from the STO side with an Al in the LAO. The results are shown in Fig. 11. On the right of this figure, we show the model indicating in which layer the $\rm Ti_{Al}$ and $\rm Al_{Ti}$ are placed. In the middle we show the layer buckling after relaxation and on the right the PDOS. The corresponding electrostatic potential profiles are shown in Fig. 10. We considered two cases: in both the $\rm Ti_{Al}$ occurs in the $\rm AlO_2$ layer closest to the interface. In model (a), the $\rm Al_{Ti}$ is placed deeper into the STO region, one $\rm TiO_2$-layer removed from the interface layer, in model (b) it is placed in the interface $\rm TiO_2$-layer. First we note that both the Al and Ti were displaced away from the interface. Their displacements relative to the O in their plane were 0.15 Å for the $\rm Ti_{Al}$ compared to 0.14 Å for the Al in the same layer. For the $\rm Al_{Ti}$ on the STO side, the displacement relative to the oxygen was -0.03 Å compared to -0.02 Å for Ti in that layer.

The results are similar to the previous case where we only added Ti. One can see that the $\rm Ti_{Al}$ PDOS in the Al layer is located at about 2 eV above the Fermi level, well above the CBM of STO. Thus their electron is transferred to the STO. However, the $\rm TiO_2$ layer on the STO now lacks an electron by having one Ti replaced by Al, and thus no electrons accumulate in the STO. This is true in both models, neither of which show a 2DEG. In the case where the Al is place deeper into the STO, one can see that the electrostatic potential is higher in that layer by the energy shift of the local PDOS.

The dipoles related to the swap and corresponding atomic displacements are such that the potential slope is reduced or taken care of within the near interface region, as can be seen in Fig. 10. The three cases all show a more or less flat potential in the LAO region near the interface and a sloped potential near the surface. We can also see changes in the potential on the STO region of the interface. Depending on how deep the Al is placed, the potential slope in the interface region becomes more spread out. As expected the interdiffusion widens the interface region.

In summary, the $\rm Ti_{Al}$ in the LAO appears in each case to donate its electrons to the interface or STO region rather than forming $\rm Ti^{3+}$ in its own layer. However, if we also place Al on the STO side as would occur in actual interdiffusion without Ti enrichment, then the Al on the STO side compensates the added electrons and no 2DEG results. Nonetheless, the linear potential variation

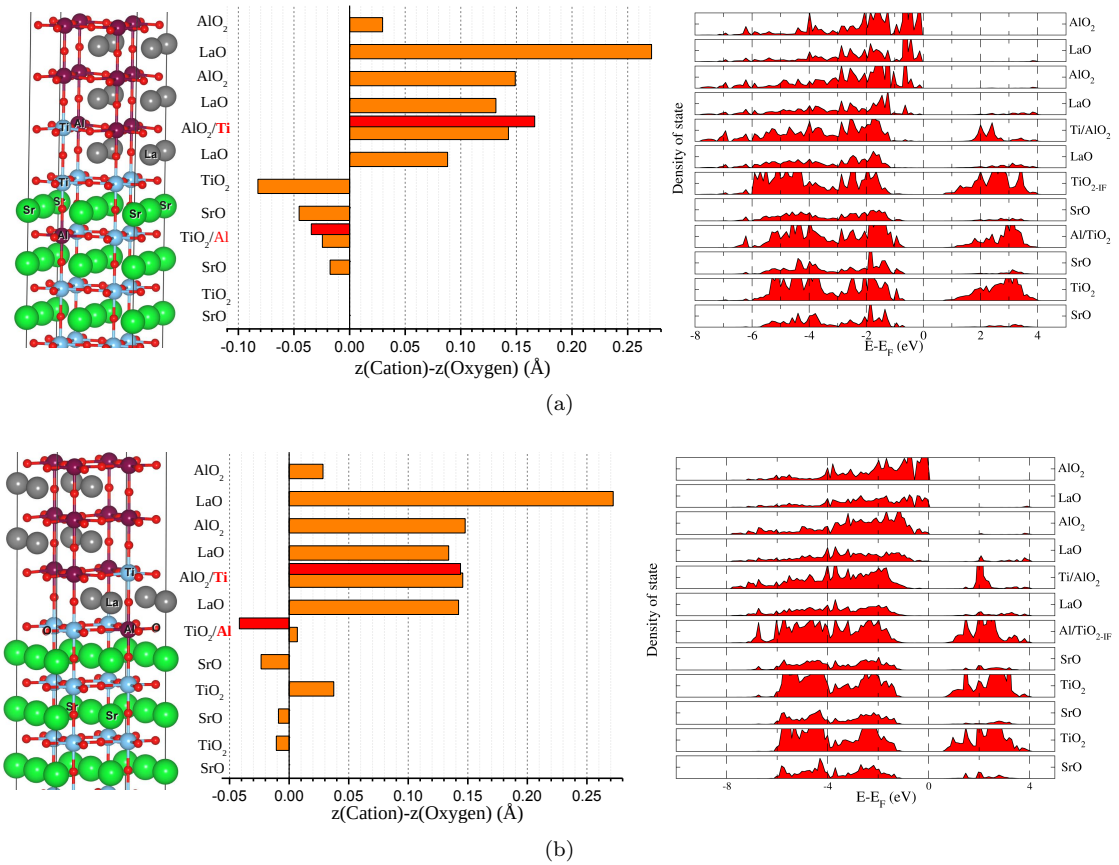

FIG. 11. (Color on-line) Structural model (left), buckling of layers (middle) and PDOS (right) for two Ti-Al intermixing models. The bar graphs show $\Delta z = z_{\rm oxygen} - z_{\rm cation}$ with z the distance normal to the interface. In (a) the Al_{Ti} is placed in the subinterface TiO_2 layer, in (b) it is in the interface layer.

of the models without interdiffusion are no longer seen. The dipoles induced by the atomic displacements modify the potential profile and eliminate the overall slope in the near interface region. However, a potential slope remains in the surface region and leads to a surface like state decay of the AlO_2 PDOS. In other words, there is a surface band bending effect.

E. Sr-La interdiffusion effects.

In this section, we present our results for Sr-La interdiffusion effects as studied in the same 3 LAO layer 2×2 2D supercell case. The results are shown in Fig. 12.

In the first example we place Sr_{La} in the LAO layer right next to the interface and La_{Sr} in the first SrO layer next to the TiO_2 interface layer. In terms of the structure, we find that Sr_{La} moves less toward the surface from its oxygen layer than the La in the same layer. In other words, relative to the La, the Sr moves closer to the interface. This trend is opposite to that of Ti_{Al} in the previous section. The PDOS shows that no 2DEG forms.

As a second Sr-Al swap case we placed the Sr_{La} in the LaO layer farther away from the interface, in fact in the middle LaO layer, but kept the La_{Sr} in the SrO layer next to the TiO_2. The Sr_{La} was still found to move toward the interface relative to the La but slightly less so than in the near surface layer, studied in the previous case. Remarkably in this case we do find an interface state in the TiO_2 interface layer and formation of a 2DEG. Apparently just shifting the Sr_{La} one layer further away from the interface results in a somewhat different electrostatic potential profile which allows some of the surface charge to transfer to the TiO_2. It should be noted that in this case the Sr_{La} lies in the middle of the 3 layer LAO film and in some sense allows the surface to communicate with the interface, whereas in the previous case, the slope potential and any charge transfer was restricted to the near interface region. The net sheet density, in this case however is found to be only 6×10^{12} e/cm^2.

The potential profile for both Sr_{La} positions is shown in Fig. 13. For the case of Sr close to the interface, shown by dashed red line, the profile is smooth and shows a flat region in the center of the LAO layer. For the Sr_{La} farther away form the interface, shown by dashed-dotted blue line, the profile is more complex with a vanishing slope at about 49 Å and another one at about 44 Å.

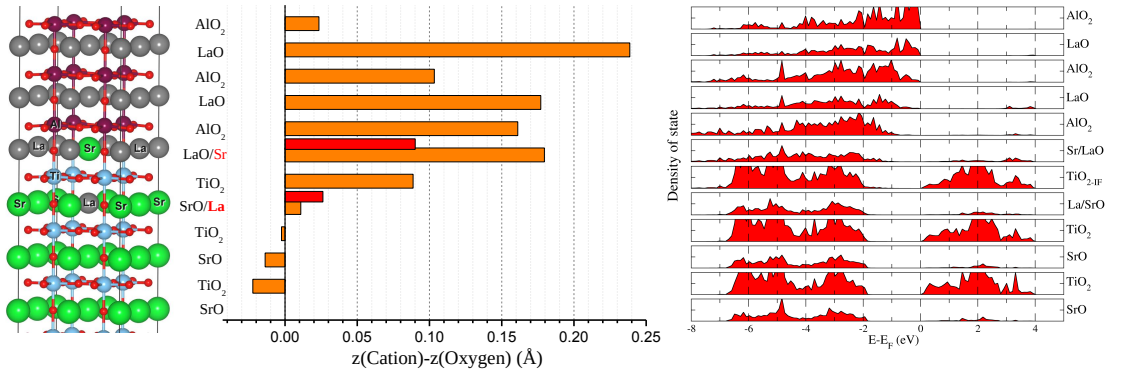

(a)

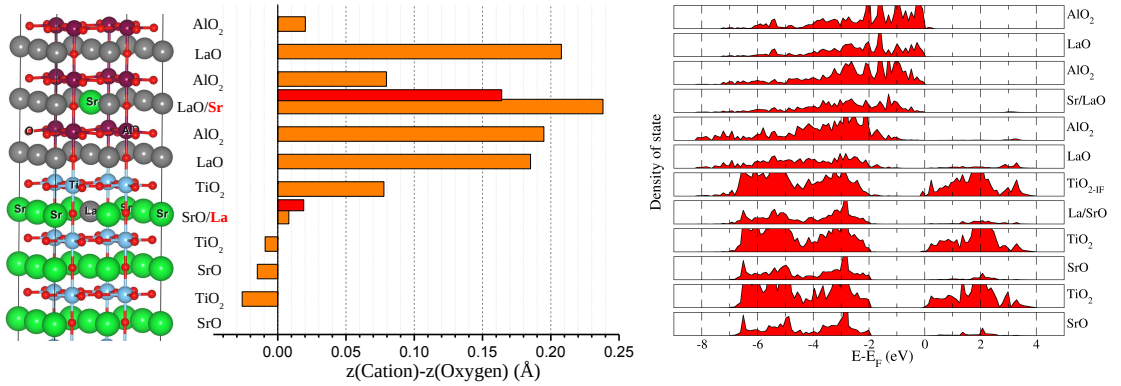

(b)

FIG. 12. (Color on-line) Structural model (left), buckling of layers (middle) and PDOS (right) for two Sr-La interdiffusion models. The bar graphs show $\Delta z = z_{\text{oxygen}} - z_{\text{cation}}$ with z the distance normal to the interface. In case (a) Sr_{La} occurs closer to the interface than in case (b).

Overall the slopes in potential in the LAO region are reduced compared to the model without any interdiffusion (shown as solid black line) but the effect of the valence discontinuity is not entirely removed.

In summary of this section, the situation for a Sr-La swap the situation is slightly more complex. Essentially the dipoles help adjust the potential slope in the near interface region. However, the Sr_{La} may also contribute to the 2DEG formation if it lies in the middle of the LAO region. The variations in electrostatic potential layer by layer in that case seem to facilitate some charge transfer from surface to interface. The potential in the mixed Sr-La layer is raised and thereby the surface state extends deeper into the LAO region from the surface and allowed charge to be transferred to the interface. However, the contribution to the sheet density was found to be smaller than for the other mechanisms discussed in the previous sections.

IV. CONCLUSIONS

In this paper we studied various models of LAO/STO interfaces with the goal of evaluating different possible mechanisms to avoid the polar discontinuity with or without formation of a 2DEG or electronic reconstruction. Our main conclusions can be summarized as follows.

First, we studied abrupt LAO/STO interface models with bare surfaces and without any interdiffusion. In agreement with previous work we find a critical layer thickness for formation of a 2DEG of 4 layers of LAO. We also determined quantitatively the electron density in the 2DEG and studied its spread over the STO layers. We find a 2DEG concentration in the order of 10^{13} e/cm^2 in qualitative agreement with experiment and also studied how this affects the slopes of the potential that remain near the interface. The 2DEG concentrations for the various cases studied are summarized in Table I.

We also analyzed the contributions of the lattice relaxation to this problem. The displacements are such as to reduce the potential slope. A larger sheet density is found for the 5-LAO layer case than the 4-LAO layer case and this results in a different orbital character of the states contributing to the 2DEG. In the 4-LAO layer case, only d_{xy} like states are occupied while in the 5-LAO layer case, d_{xy} like states are occupied near the interface but in addition d_{xz} and d_{yz} like states are also partially occupied in the deeper STO layers.

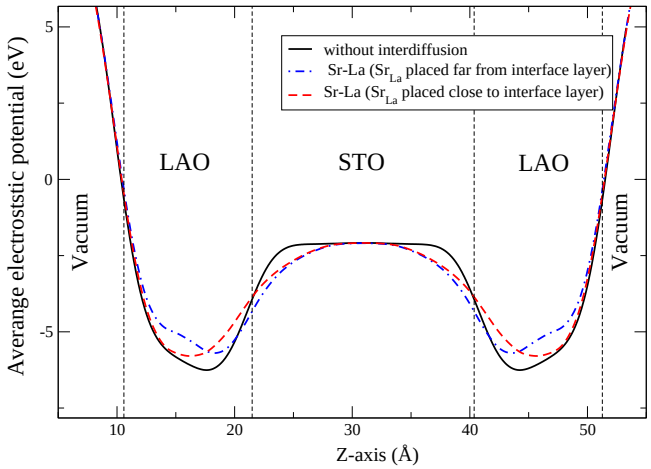

FIG. 13. (Color on-line) Macroscopically averaged electrostatic potentials for two cases of Sr-La interdiffusion compared with the case of no interdiffusion. The vertical dashed lines show the positions of the interface and surface layers.

TABLE I. Summary of occurrence of 2DEG and its interface sheet density σ for various cases

system	2DEG	σ (10^{13} e/cm^2)
3-LAO-layer	No	
4-LAO-layer	Yes	1.43
5-LAO-layer	Yes	2.14
3-LAO+$\frac{1}{8}$H-coverage	Yes	1.20
3-LAO+$\frac{1}{2}$H-coverage	Yes	2.88
3-LAO+ full H coverage	Yes	3.01[a]
4-LAO+ full H coverage	Yes	9.00
3-LAO+$\frac{1}{4}$ Ti_{Al}	Yes	1.10
3-LAO+$\frac{1}{4}$ Ti_{Al} + Al_{Ti}	No	
3-LAO+$\frac{1}{4}$ Sr_{La} at interface + La_{Sr}	No	
3-LAO+$\frac{1}{4}$ Sr_{La} in middle LAO + La_{Sr}	Yes	0.6

[a] In this case, a surface 2DEG of 6.2×10^{13} e/cm^2 is also present.

Next, we studied surface termination effects or surface passivation effects by water absorption. We did this for the situation of a below critical thickness LAO layer of only 3 unit cells thick. We find first that H_2O absorbed on Al prefers to split into OH on Al and H on surface O. We found that H on O donates its electrons to the interface rather than forming surface states in the AlO_2 layer. However, this is only true if the H concentration is not too high. Here we studied only two limiting cases, a low coverage of 1/8 H restricted by the size of cell we can deal with and a high coverage of 1 H per surface O. In the latter case, the potential slope problem is reversed and a significant electron density is found in surface states below the LAO CBM.

Adsorption of OH on the Al on the other hand leads to a p-type surface and with acceptor like surface states above the LAO VBM. This does not help to reduce the polar discontinuity potential and in fact compensates the H 2DEG if both are present simultaneously.

Finally we studied both Ti-Al and Sr-La interdiffusion effects. We found that Ti_{Al} and Al_{Ti} tend to be displaced away from the interface. These dipoles already would help reduce the potential slope resulting from the polar discontinuity. On the other hand, Ti_{Al} is found not to convert to Ti^{3+} but rather to donate its electrons to the STO. If there is excess Ti and the STO remains unmixed, the polar discontinuity is avoided and a sizable 2DEG concentration is achieved. On the other hand, if the Ti_{Al} is compensated by an Al_{Ti} in the STO TiO_2 interface layer, then the extra Al on the TiO_2 layer contributes a compensating hole so that no net 2DEG forms. A significant surface potential bending remains in the LAO layer leading to a surface state like decay of the LaO and AlO_2 layer PDOS.

For Sr-La interdiffusion we found that both Sr_{La} and La_{Sr} tend to be displaced toward the interface. Both Sr and La are merely donors in their respective crystals and so do not contribute relevant energy levels near the VBM or CBM. The nuclear charge swaps simply compensate and no 2DEG forms if both are close to the interface. However, we found that they nonetheless affect the electrostatic potentials in the layers in which they reside. Thereby they can influence the potential profile and for example for Sr_{La} placed in the middle of the 3layer LAO, we found that it helped transferring charge from the surface to the interface so that now a 2DEG formed even for a layer thickness below the normal critical layer thickness.

Although some interesting and unexpected effects of the interdiffusion were found here, we caution that a full study of this would require a statistical averaging and taking into account how much actual interdiffusion takes place and how the interdiffused atoms are distributed over the layers. Such information is recently becoming available from MEIS studies by Zaid *et al.*[2] However, the gradual interdiffusion profile is too complex to treat directly with first-principles simulations. A small concentration in a any given layer would require a much large 2D cell than we here can afford with present computational power. Secondly, some of the effects we found here could compensate each other. Therefore the value of the present results lies more in the qualitative findings. A fully quantitative treatment of these various effects on the 2DEG electron density requires probably a simpler modeling approach in which some of these qualitative aspects are incorporated.

Still, some of our predictions are worthwhile further testing experimentally, in particular the prediction that Ti_{Al} on the LAO side after interdiffusion would stay Ti^{4+}. In both cases, of course it contributes to the overall 2DEG electron density but our calculation predicts the latter should stay confined to the STO rather than making the whole LAO film n-type doped.

ACKNOWLEDGMENTS

This work was supported by the U.S. Air Force Of-

fice of Scientific Research under Grant No. FA9550-12-1-0441. One of the authors (I. F.) was supported by the Development and Promotion of Science and Technology Talents Project(DPST). S. L. and I. F. acknowledge the support from the NANOTEC-SUT Center for Excellence on Advanced Functional Nanomaterials. The calculations used the High Performance Computing Resource in the Core Facility for Advanced Research Computing at Case Western Reserve University.

[1] A. Ohtomo and H. Y. Hwang, Nature **427**, 422 (2004).
[2] H. Zaid, M. Berger, D. Jalabert, M. Walls, N. G. R. Akrobetu, X. Gao, P. Berger, I. Fongkaew, W. R. L. Lambrecht, and A.Sehirlioglu, "Atomic-resolved depth profile of strain and cation intermixing around $LaAlO_3/SrTiO_3$ interfaces." (2015), unpublished.
[3] R. Pentcheva and W. E. Pickett, Phys. Rev. B **78**, 205106 (2008).
[4] R. Pentcheva and W. E. Pickett, Phys. Rev. Lett. **102**, 107602 (2009).
[5] A. Janotti, L. Bjaalie, L. Gordon, and C. G. Van de Walle, Phys. Rev. B **86**, 241108 (2012).
[6] Z. S. Popović, S. Satpathy, and R. M. Martin, Phys. Rev. Lett. **101**, 256801 (2008).
[7] H. Chen, A. Kolpak, and S. Ismail-Beigi, Phys. Rev. B **82**, 085430 (2010).
[8] Z. Zhong, P. X. Xu, and P. J. Kelly, Phys. Rev. B **82**, 165127 (2010).
[9] R. Pentcheva and W. E. Pickett, Phys. Rev. B **74**, 035112 (2006).
[10] L. Yu and A. Zunger, Nature Communications **5**, 5118 (2014).
[11] Y. Li, S. N. Phattalung, S. Limpijumnong, J. Kim, and J. Yu, Phys. Rev. B **84**, 245307 (2011).
[12] L. Zhang, X.-F. Zhou, H.-T. Wang, J.-J. Xu, J. Li, E. G. Wang, and S.-H. Wei, Phys. Rev. B **82**, 125412 (2010).
[13] J. Lee and A. A. Demkov, Phys. Rev. B **78**, 193104 (2008).
[14] C. Cen, S. Thiel, G. Hammerl, C. W. Schneider, K. E. Andersen, C. S. Hellberg, J. Mannhart, and J. Levy, Nature Mater. **7**, 298 (2008).
[15] C. Cen, S. Thiel, J. Mannhart, and J. Levy, Science **323**, 1026 (2009), http://www.sciencemag.org/content/323/5917/1026.full.pdf.
[16] G. Cheng, P. F. Siles, F. Bi, C. Cen, D. F. Bogorin, C. W. Bark, C. M. Folkman, J.-W. Park, C.-B. Eom, G. Medeiros-Ribeiro, and J. Levy, Nature Nanotechnology **6**, 343 (2011).
[17] G. Cheng, J. P. Veazey, P. Irvin, C. Cen, D. F. Bogorin, F. Bi, M. Huang, S. Lu, C.-W. Bark, S. Ryu, K.-H. Cho, C.-B. Eom, and J. Levy, Phys. Rev. X **3**, 011021 (2013).
[18] F. Bi, D. F. Bogorin, C. Cen, C. W. Bark, J.-W. Park, C.-B. Eom, and J. Levy, Applied Physics Letters **97**, 173110 (2010).
[19] P. E. Blöchl, Phys. Rev. B **50**, 17953 (1994).
[20] G. Kresse and D. Joubert, Phys. Rev. B **59**, 1758 (1999).
[21] G. Kresse and J. Furthmiiller, Computational Materials Science **6**, 15 (1996).
[22] G. Kresse and J. Hafner, Journal of Physics: Condensed Matter **6**, 8245 (1994).
[23] G. Kresse and D. Joubert, Phys. Rev. B **59**, 1758 (1999).
[24] J. P. Perdew, K. Burke, and M. Ernzerhof, Phys. Rev. Lett. **78**, 1396 (1997).
[25] J. P. Perdew, K. Burke, and M. Ernzerhof, Phys. Rev. Lett. **77**, 3865 (1996).
[26] D. Vanderbilt, Phys. Rev. B **41**, 7892 (1990).
[27] R. P. Feynman, Phys. Rev. **56**, 340 (1939).
[28] H. J. Monkhorst and J. D. Pack, Phys. Rev. B **13**, 5188 (1976).
[29] S. Thiel, G. Hammerl, A. Schmehl, C. W. Schneider, and J. Mannhart, Science **313**, 1942 (2006), http://www.sciencemag.org/content/313/5795/1942.full.pdf.
[30] M. Reinle-Schmitt, C. Cancellieri, D. Li, D. Fontaine, M. Medarde, E. Pomjakushina, C. Schneider, S. Gariglio, P. Ghosez, J.-M. Triscone, and P. Willmott, Nat. Commun. , 932 (2012).